JOURNAL OF SOLID STATE CHEMISTRY **103**, 152–159 (1993)

Magnetic and Crystal Structure Determination of K_2UBr_5

KARL KRÄMER,*,† LUKAS KELLER,‡ PETER FISCHER,‡
BERND JUNG,§ NORMAN N. EDELSTEIN,§ HANS-U. GÜDEL,†
AND GERD MEYER*

**Institut für Anorganische Chemie, Universität Hannover, Callinstrasse 9, W-3000 Hannover, Germany; †Institut für Anorganische, Analytische und Physikalische Chemie, Universität Bern, Freiestrasse 3, CH-3000 Bern, Switzerland; ‡Labor für Neutronenstreuung, Eidgenössische Technische Hochschule Zürich, CH-5232 Villigen PSI, Switzerland; and §Lawrence Berkeley Laboratory, University of California, 1 Cyclotron Road, Berkeley, California 94720*

Received May 28, 1992; in revised form August 10, 1992; accepted August 12, 1992

Magnetic susceptibility measurements show an antiferromagnetic ordering phenomenon for K_2UBr_5. There is a broad maximum in the χ versus T curve at about 10 K. Aiming at the determination of the magnetic structure of K_2UBr_5, powder neutron diffraction investigations were performed. The nuclear structure of K_2UBr_5 (K_2PrCl_5 type of structure) was refined at 15 K in the paramagnetic state. The magnetic structure, which was determined from a measurement at 1.5 K in the magnetically ordered state, belongs to the Shubnikov space group $Pn'm'a'$ with $\mathbf{k} = 0$. In the uranium chains along [010] there is an antiferromagnetic ordering of the magnetic moments with components in the (010) plane only. The magnetic moments of neighboring chains are perpendicular to each other within the error limit. Each U^{3+} has an ordered magnetic moment of 2.31(4) μ_B. According to the temperature dependence of the intensity of the 010 and 111 magnetic peaks the Néel temperature is 2.8(3) K. Presumably, there is a short-range magnetic ordering along the $[UBr_3Br_{4/2}]^{2-}$ chains giving rise to the maximum of χ at $T = 10$ K, followed by long-range (three-dimensional) ordering at 2.8 K.

Introduction

Many uranium(III) halides undergo magnetic phase transitions at low temperatures; most of them order antiferromagnetically. The Néel temperatures T_N depend on the U–U distances and the structure type. For a number of compounds, bulk magnetic measurements are available. Magnetic structure determinations have so far only been carried out for binary halides UX_3 (*1*), such as UCl_3 (*2*), UBr_3 (*3*), and UI_3 (*4*).

The ternary uranium(III) halides A_2UX_5 with A = K, Rb and X = Cl, Br, I adopt the K_2PrCl_5 type of structure (*5*), as was shown for the chlorides (*6*) and recently for the bromides and iodides (*7*). Bulk magnetic measurements of the chlorides A_2UCl_5 (A = K, NH_4, Rb) (*8*) give evidence for antiferromagnetic ordering. However, a first attempt to determine the magnetic structure of K_2UCl_5 (*9*) was not successful because of limited sample quality. Here we report the first magnetic structure of a ternary uranium(III) halide.

0022-4596/93 $5.00

Experimental

K_2UBr_5 was prepared from the binary components KBr and UBr_3 (*7*) in tantalum containers which were sealed gas tight by helium arc welding (*10*) and jacketed with silica tubing. The containers were heated to 760°C for 1 day and over 1 week slowly cooled to 560°C, after which the power to the furnace was turned off. K_2UBr_5 and UBr_3 are very sensitive to moisture and oxidation. Therefore, all preparative steps and sample handling were carried out under strictly dry and anaerobic conditions, making use of vacuum/inert gas techniques and argon glove boxes. The quality of the K_2UBr_5 samples was checked by X-ray Guinier diffraction. The pattern could be indexed completely; impurity lines were not detected.

For neutron scattering experiments the ground powder was filled into a vanadium container (ϕ 8 mm, length 50 mm) under a helium atmosphere. The measurements were performed on the diffractometers DMC (*11*) and 2AX at reactor Saphir of the Paul Scherrer-Institut (Villigen, Switzerland) using "ILL-type" helium gas flow cryostats. The nuclear structure was refined at 15 K in the paramagnetic state from DMC data (λ = 170.12 pm, high resolution mode) using the Young–Wiles program (*12*). Further measurements were performed on DMC in the high intensity mode (λ = 170.08 pm) at 1.5 and 15 K. From the pattern at 1.5 K and the difference pattern 1.5–15 K the magnetic structure of the ordered state was calculated by a Rietveld program (*13*). All DMC measurements were corrected for absorption according to the measured transmission (μ = 0.363 cm^{-1} for λ = 170.08 pm). For the calculations the neutron scattering lengths published by Sears (*14*) and a calculated relativistic neutron magnetic form factor for U^{3+} (*15*) were used. The temperature dependence of the magnetic Bragg peaks 010 and 111 were determined on the two-axis diffractometer 2AX (λ = 233.7 pm) between 1.4 and 12 K.

The magnetic susceptibility of K_2UBr_5 was measured with a SHE (model 905) SQUID magnetometer. Two different samples were measured, each at 0.5 and 4 T: one in the temperature range 5–300 K, and the second from 2–300 K. Each sample was powdered and placed in a sealable Kel F container. Data were corrected for diamagnetic contributions of the Kel F container and of the K_2UBr_5.

Results and Discussion

The magnetic susceptibility of K_2UBr_5 shows an antiferromagnetic behaviour. There is a broad maximum in the χ versus T curve at about 10 K (Fig. 1). A second measurement of the magnetic susceptibility down to 2 K possibly showed a weak feature below 3 K indicative of three-dimensional magnetic ordering. The susceptibility decreases to χ = 0.02 emu/mol at 2 K. A linear regression of the paramagnetic data between 40 and 300 K according to the Curie–Weiss law yields a Weiss constant of $\theta = -15(1)$ K which indicates an antiferromagnetic nearest-neighbor interaction. From the Curie constant C = 1.55(1) emu · K/mol an effective magnetic moment of $\mu_{eff} = 3.52(1)\ \mu_B$ for U^{3+} is obtained.

K_2UBr_5 belongs to the K_2PrCl_5 type of structure (*5*) as previously reported (*7*). The results of the structure refinement in the paramagnetic state at 15 K by the Young–Wiles program (DMC, high resolution data) are summarized in Table I. They are consistent with the single-crystal structure determination of isotypic K_2UI_5 and lattice constants derived from the X-ray Guinier powder pattern of K_2UBr_5 at room temperature (*7*). K_2UBr_5 contains chains of $[UBr1Br2Br3Br4_{4/2}]^{2-}$ polyhedra parallel to the b-axis with sevenfold coordinate U^{3+} (distorted pentagonal bipyramides; Fig. 2). The chains are far away from each other,

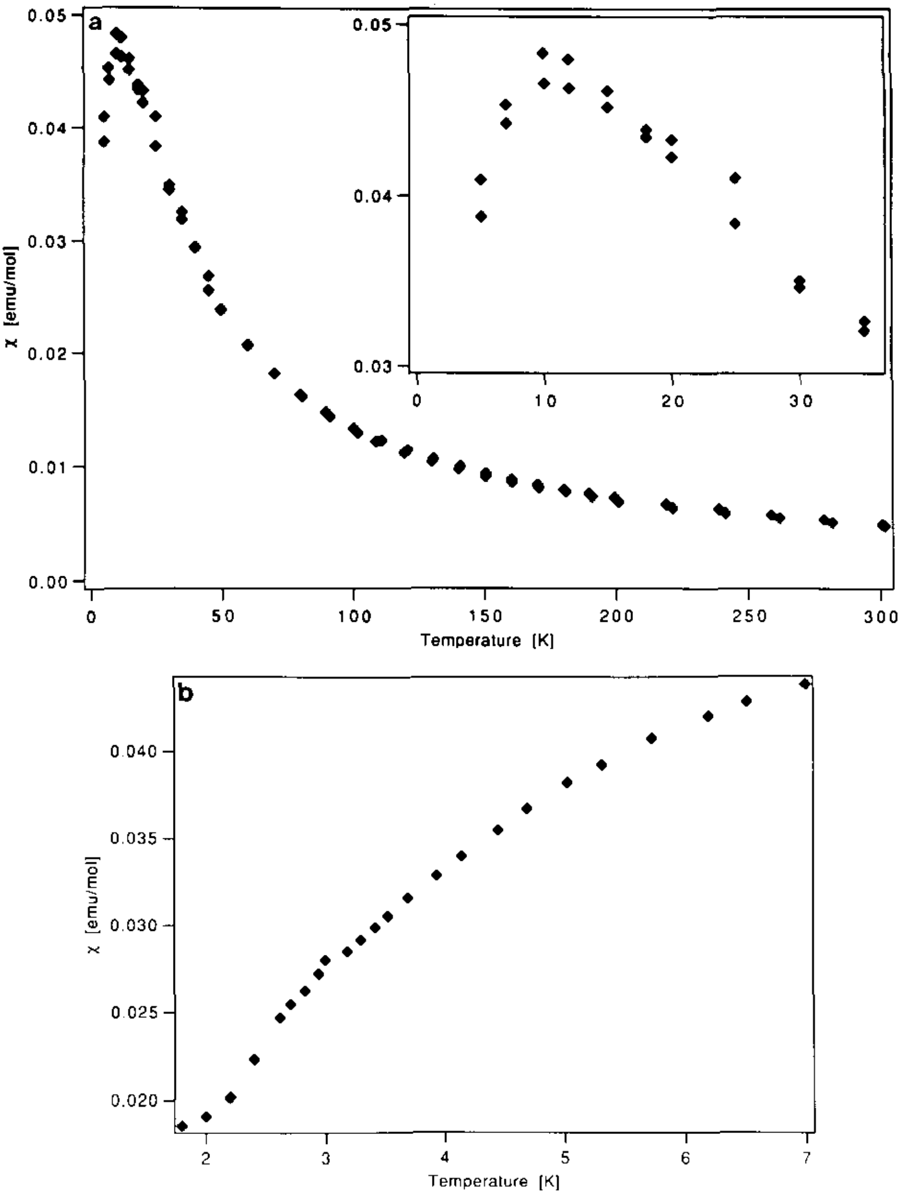

FIG. 1. Temperature dependence of the magnetic susceptibility of K_2UBr_5 (0.5 T): (a) 5–300 K, (b) 2–7 K.

separated by potassium ions (Fig. 3). The U–U distances within a chain are 478.2 pm while the shortest distances between neighbouring chains are 718.4 pm for U(1)–U(4) and U(2)–U(3). Interatomic distances, which are consistent with values known for K^+, U^{3+} and Br^- separations, are summarized in Table II.

The long-range magnetic structure of K_2UBr_5 at 1.5 K was determined by means

TABLE I

CRYSTALLOGRAPHIC DATA OF K_2UBr_5 AT 15 K DERIVED FROM A DMC MEASUREMENT (λ = 170.12 pm, HIGH RESOLUTION MODE) BY THE YOUNG–WILES PROGRAM

Lattice constants/pm: a = 1321.2(1) b = 916.42(7) c = 836.19(6)
Crystal system: orthorhombic, space group: *Pnma* (No. 62), Z = 4
Number of inequivalent reflections: 1215
Agreement values /%: R_{wp} = 5.9, R_{exp} = 3.9, R_p = 4.5
Atomic positions and isotropic temperature factors B (Å^2):

Atom	Site	x/a	y/b	z/c	B
K	(8d)	0.6730(6)	0.4963(12)	0.5535(10)	0.7(2)
U	(4c)	0.5062(6)	0.25	0.0812(7)	0.6(1)
Br1	(4c)	0.9947(6)	0.75	0.9375(8)	0.5(2)
Br2	(4c)	0.7889(5)	0.25	0.3290(9)	0.5(2)
Br3	(4c)	0.6843(5)	0.25	0.8688(8)	0.4(2)
Br4	(8d)	0.5791(4)	0.5466(5)	0.1710(7)	0.4(1)

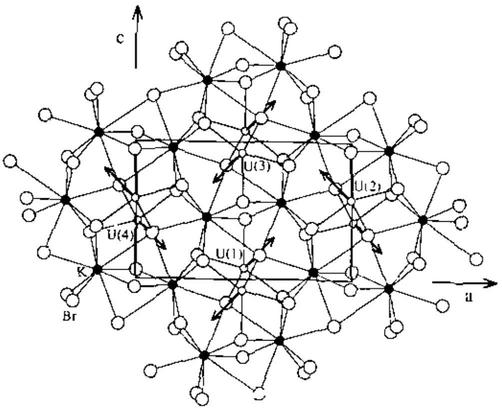

FIG. 3. View onto the (010) plane of K_2UBr_5.

of a Rietveld program from the DMC data at 1.5 K (Fig. 4b) and the difference pattern 1.5–15 K (Fig. 4c) which shows the magnetic contributions to the scattering pattern. In the ordered state, a great number of magnetic Bragg peaks occur (Fig. 4c) which were all indexed in terms of the nuclear cell, i.e., $\mathbf{k} = 0$. The strongest magnetic reflections (010 at 2θ = 10.7° (λ = 170.08 pm), 110 at 13.0°, 111 at 17.5°, 211 at 21.8°, 310 at 24.8° and 131 at 35.4°) correspond to a $k = 2\,n + 1$ rule, but the rule is broken by many weak ones. Thus, a predominant antiferromagnetic ordering along the b-axis may be derived.

For the magnetic calculations, the nuclear parameters of the paramagnetic state at 15 K were used and kept fixed and the two magnetic structure parameters (μ_x, μ_z) were refined. Magnetic contributions to the scattering pattern were included up to 2θ = 40° (λ = 170.08 pm). The best fit of calculated and observed powder patterns was achieved for the Shubnikov space group $Pn'm'a'$. The R-value obtained for $Pn'm'a'$ is two to three times better than those for other magnetic space groups. The uranium ions occupy the special site (4c) with site symmetry (.m.) in *Pnma*. In $Pn'm'a'$ the symmetry of site (4c) changes to an anti-mirror plane (.m'.) with the result that the magnetic moments may

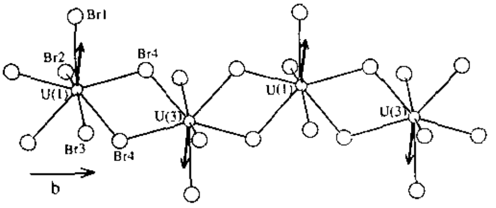

FIG. 2. Chain of uranium polyhedra $[UBr1Br2Br3Br4_{4/2}]^{2-}$ of K_2UBr_5 along [010].

TABLE II

INTERATOMIC DISTANCES [pm] IN K_2UBr_5 AT 15 K

d(U–Br1)	= 297.9	d(K–Br1)	= 330.8 331.1
d(U–Br2)	= 296.8	d(K–Br2)	= 331.1 331.1
d(U–Br3)	= 294.8	d(K–Br3)	= 336.8 347.4
d(U–Br4)	= 298.0 (2×) 303.2 (2×)	d(K–Br4)	= 344.2 346.1 406.9
$\bar{d}$(U–Br)	= 298.8	$\bar{d}$(K–Br)	= 345.1
d(U–U)	= 478.2	Intrachain distance U(1)–U(3), U(2)–U(4)	
	718.4	Shortest interchain distance U(1)–U(4), U(2)–U(3)	

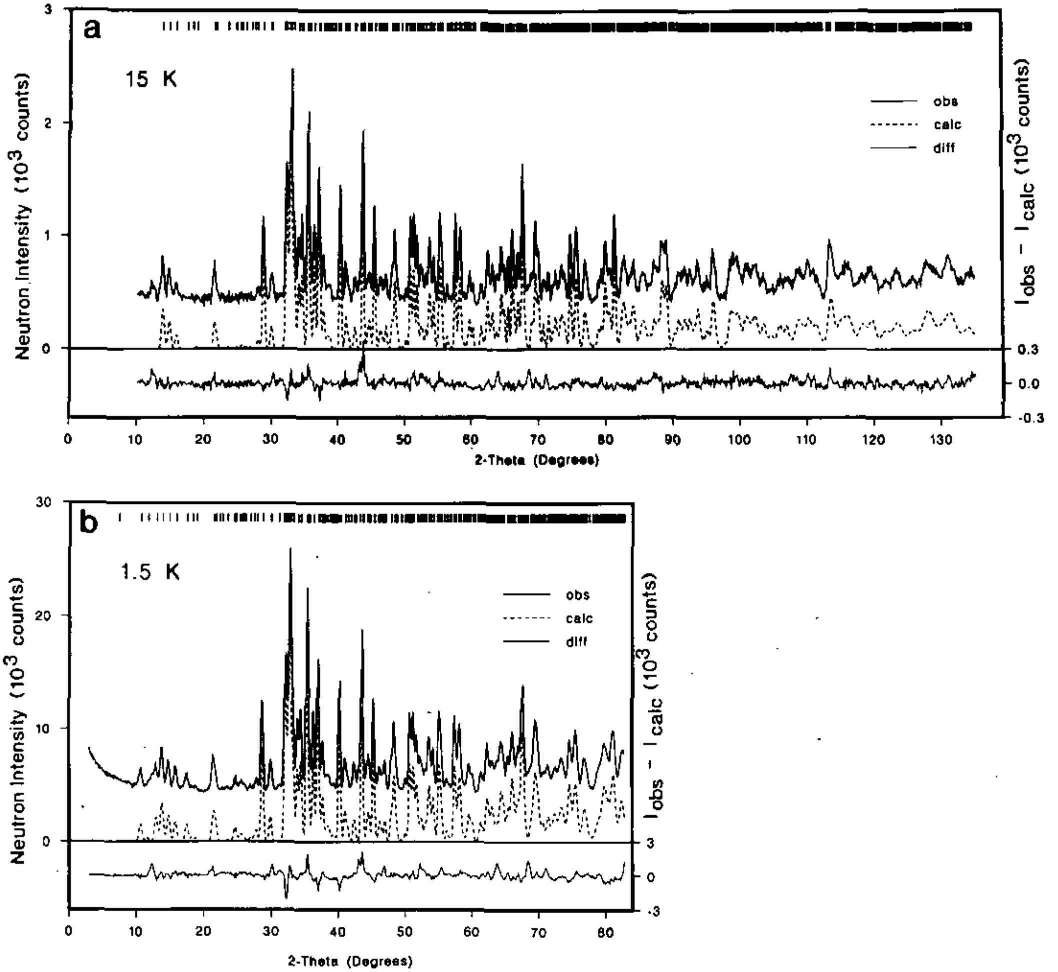

FIG. 4. Observed, calculated and difference neutron diffraction patterns of (a) paramagnetic K_2UBr_5 at 15 K(DMC, high resolution mode, λ = 170.12 pm), (b) magnetically ordered K_2UBr_5 at 1.5 K (DMC, high intensity mode, λ = 170.08 pm), and (c) difference pattern 1.5–15 K of K_2UBr_5 (DMC, high intensity mode, λ = 170.08 pm).

have components along the *a*- and *c*-axes only. The calculations in *Pn'm'a'* result in an ordered magnetic moment of 2.31(4) μ_B/U^{3+} with components of μ_x = 1.66(4) μ_B and μ_z = 1.60(4) μ_B which are equal within the error limits (Table III). The ordered magnetic moment is remarkably reduced below the saturation value of $g \cdot J$ = 3.26 μ_B for U^{3+} in a $^4I_{9/2}$ state. Responsible for this reduction are the crystal field and possibly zero-point fluctations typically found in one-dimensional magnetic systems. We have not attempted to calculate the effect of the crystal field on the free U^{3+} ion ground state. The situation is rather difficult due to the sevenfold coordination and the low point symmetry (*.m.*) of U^{3+} which will split up the $^4I_{9/2}$ ground state into 5 Kramer's dublets. A reduction of the ordered magnetic moment has also been ob-

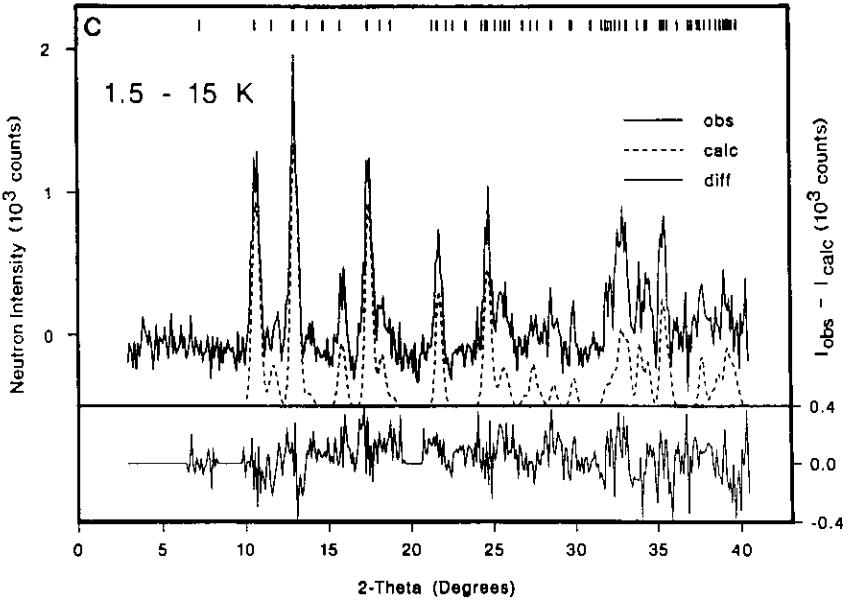

FIG. 4—*Continued*

served in $CsVX_3$ (*17*) and $CsMnBr_3$ (*18*) (see below). In both references the reduction was ascribed to zero-point fluctuations. The U^{3+} chains parallel to the *b*-axis, which consist of U(1)–U(3) resp. U(2)–U(4), are ordered antiferromagnetically (Fig. 2). The magnetic moments of neighboring chains, i.e. U(1)–U(3) versus U(2)–U(4), are perpendicular to each other within the error limits (Fig. 3).

To determine the three-dimensional ordering temperature, the neutron intensities of the magnetic 010 and 111 Bragg reflections were measured between 1.4 and 12 K on the 2AX diffractometer. Despite the broad maximum in the χ versus T curve at 10 K (Fig. 1), Fig. 5 clearly shows that the three-dimensional ordering temperature is $T_N = 2.8(3)$ K. Apparently, there is a short-range magnetic ordering giving rise to the maximum of χ at about 10 K followed by a long-range (three-dimensional) ordering at 2.8 K as described above. The three-dimensional ordering, which can be detected clearly by neutron scattering, can hardly be seen in magnetic susceptibility measurements. The one-dimensional ordering aligns the magnetic moments to such an extent that the effect of the three-dimensional alignment on the magnetic susceptibility will be very weak.

From the structural point of view, the short-range ordering must be one-dimen-

TABLE III

MAGNETIC DATA OF K_2UBr_5 AT 1.5 K DERIVED FROM THE DIFFERENCE PATTERN 1.5–15 K OF THE DMC MEASUREMENTS ($\lambda = 170.08$ pm, HIGH INTENSITY MODE) BY THE RIETVELD PROGRAM

Shubnikov space group: *Pn′m′a′*, $\mathbf{k} = 0$
$R_{mag} = 18.46\%$
Coordinates and components of the ordered magnetic moments of U^{3+}:

	x/a	y/b	z/c	μ_x/μ_B	μ_y/μ_B	μ_z/μ_B
U(1)	0.5062	0.25	0.0812	1.66(4)	0	1.60(4)
U(2)	0.9938	0.75	0.5812	−1.66	0	1.60
U(3)	0.4938	0.75	0.9188	−1.66	0	−1.60
U(4)	0.0062	0.25	0.4188	1.66	0	−1.60

$\mu(U^{3+}) = 2.31(4)\ \mu_B$

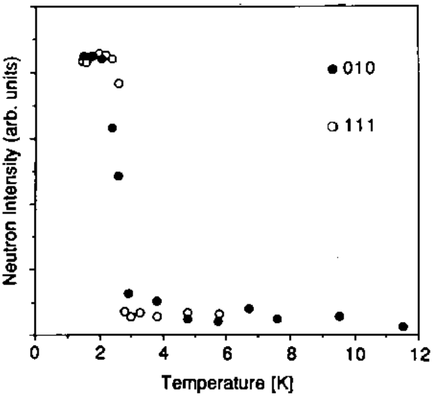

FIG. 5. Temperature dependence of the neutron peak counts of the 010 and 111 Bragg reflections in K_2UBr_5 (2AX).

sional along the U^{3+} chains with a negative (antiferromagnetic) exchange interaction. The interchain interaction leading to the three-dimensional ordering below 2.8 K acts in the (010) plane with a positive (ferromagnetic) exchange parameter. The ordered magnetic moments in the (010) plane, i.e., U(1) + U(4) and U(2) + U(3), do not add to zero, because they are perpendicular to each other. Thus the z-components disappear but the x-components add to $\mu_x = 3.22$ μ_B and $\mu_x = -3.32$ μ_B for U(1) + U(4) and U(2) + U(3), respectively (see Table III). Nevertheless, the overall magnetic moment of the unit cell disappears because of the antiferromagnetic intrachain coupling.

A behavior similar to K_2UBr_5 is known for compounds of the general composition AMX_3 (A = alkali metal ion, M = divalent transition metal ion, X = halide ion) which adopt the $CsNiCl_3$ type of structure (*16*). They crystallize in space group $P6_3/mmc$ and contain isolated $[MX_{6/2}]^-$ chains along [00.1] separated by A^+ ions. Depending on the sign and magnitude of the intra- and interchain exchange interactions, which are determined by A, M, and X, various magnetic structures are observed. $CsVX_3$ (X = Cl, Br, I) (*17*) and $CsMnBr_3$ (*18*), for example, have antiferromagnetic intra- and interchain interactions. They adopt a triangular magnetic structure in the (00.1) plane. In the compounds $AFeCl_3$ (A = Rb, Cs) (*19*) a ferromagnetic intrachain interaction was found. The binary uranium halides UX_3 (X = Cl, Br) exhibit one-dimensional ordering along the $UX_{9/3}$ chains parallel to the c-axis, followed by two transitions to three-dimensionally ordered phases (*2*, *3*).

We are currently investigating the other members of the A_2UX_5 (A = K, Rb; X = Cl, Br, I) series in order to explain the effect of the chemical variation on the magnetic properties. The three-dimensional ordering temperature is determined by the ratio of the inter- to intrachain exchange interactions. We expect opposite trends for the two interactions within the series and thus an observable effect on the ordering temperature.

Acknowledgments

This work has been supported by the Deutsche Forschungsgemeinschaft and the Bundesministerium für Forschung und Technologie, Bonn, the Fonds der Chemischen Industrie, Frankfurt/Main, and the Swiss National Science Foundation. The part of this work performed at LBL was supported by the director, Office of Energy Research, Office of Basic Energy Sciences, Chemical Sciences Division of the U.S. Department of Energy under Contract DE-AC03-76SF00098.

References

1. A. MURASIK, P. FISCHER, A. FURRER, B. SCHMID, AND W. SZCZEPANIAK, *J. Less-Common Met.* **121**, 151 (1986).
2. A. MURASIK, P. FISCHER, A. FURRER, AND W. SZCZEPANIAK, *J. Phys. C Solid State Phys.* **18**, 2909 (1985).
3. A. MURASIK, A. FURRER, AND W. SZCZEPANIAK, *Solid State Commun.* **33**, 1217 (1980).
4. A. MURASIK, P. FISCHER, AND W. SZCZEPANIAK, *J. Phys. C Solid State Phys.* **14**, 1847 (1981).
5. G. MEYER AND E. HÜTTL, *Z. Anorg. Allg. Chem.* **497**, 191 (1983). G. MEYER, J. SOOSE, A. MORITZ, V. VITT, AND TH. HOLJES, *Z. Anorg. Allg. Chem.* **521**, 161 (1985).

6. G. Meyer, H.-Chr. Gaebell, and R. Hoppe, *J. Less-Common Met.* **93,** 347 (1983).
7. K. Krämer, Dissertation, Universität Giessen (1991).
8. J. Drozdzynski and D. Miernik, *Inorg. Chim. Acta* **30,** 185 (1978).
9. Progress Report 1989, Laboratory for Neutron Scattering, Eidgenössische Technische Hochschule Zürich.
10. A. E. Miller, A. H. Daane, C. E. Habermann, and B. J. Beaudry, *Sci. Instrum.* **34,** 644 (1963); J. D. Corbett, *Inorg. Synth.* **25,** 16 (1983).
11. J. Schefer, P. Fischer, H. Heer, A. Isacson, M. Koch, and R. Thut, *Nucl. Instrum. Methods Phys. Res. Sect. A* **288,** 477 (1990).
12. D. B. Wiles and R. A. Young, *J. Appl. Crystallogr.* **14,** 149 (1981); ILL/LNS program version modified by I. Rodriguez, P. Fischer and J. Schefer.
13. H. M. Rietveld, *J. Appl. Crystallogr.* **2,** 65 (1969); A. W. Hewat, Harwell report AERE-R 7350 (1973); J. C. Howard, *J. Appl. Crystallogr.* **15,** 615 (1981).
14. V. F. Sears, "Methods of Experimental Physics" (K. Sköld and D. L. Price, Eds.), Vol. 23A, p. 599, Academic Press, London (1986).
15. A. J. Freeman, J. P. Desclaux, G. H. Lander, and J. Faber, *Phys. Rev. B* **13,** 1168 (1976).
16. M. Steiner, K. Kakurai, and J. K. Kjems, *Z. Phys. B* **53,** 117 (1983).
17. A. Hauser, U. Falk, P. Fischer, A. Furrer, and H. U. Güdel, *J. Magn. Magn. Mater.* **31–34,** 1139 (1983).
18. E. Eibschütz, R. C. Sherwood, F. S. L. Hsu, and D. E. Cox, *AIP Conf. Proc.* **10,** 684 (1972).
19. T. Haseda, N. Wada, M. Hata, and K. Amaya, *Physica B* **108,** 841 (1981).